Proceedings of the Second International Conference on Press-in Engineering 2021, Kochi, Japan – Matsumoto et al (eds)

Experimental evaluation of the lateral capacity of large jacked-in piles and comparison to existing design standards

A. Dobrisan & S.K. Haigh
Department of Engineering, University of Cambridge, Cambridge, UK

Y. Ishihara
GIKEN LTD., Kochi, Japan

ABSTRACT: The devastation caused by the 2011 Tōhoku earthquake and subsequent tsunami revealed the need for a rethink of seawall design. Along the Kochi coast a new generation of tsunami defences has been installed, consisting of large diameter adjoining steel piles with deep embedment. This paper presents the results of a full-scale lateral test on a pile identical to those used in the new seawalls. The lateral test is an optimal opportunity to check how well design codes, originally intended for smaller, flexible piles, scale-up to larger pile classes. A novel data analysis method is used to retrieve accurate p- y curves from experimental data. Results show good agreement with design p- y relationships at shallow depths, while below 3 depth the design curves significantly overpredict soil stiffness. The paper highlights the need for new, appropriate design specifications to account for large stiff piles and obtain better assessment of their lateral capacity.

1 INTRODUCTION

The devastating Tōhoku seismic event and tsunami brought about great loss of life and extensive socio-economic damage. For geotechnical engineers it highlighted the immediate need to reconsider design not just for a 100 or 200-year return period event, but for much larger, potentially never before seen, magnitudes of natural hazards.

In this light the traditional concrete caisson design of seawalls is ill suited for larger-than-planned-for events as the structure can overturn and provide no further protection to coastal areas, as happened in 2011, illustrated in Figure 1 from Kato et al. (2012).

A modern seawall design currently implemented along the Kochi coast consists of large diameter, jacked-in steel tubular piles embedded up to 15 into the ground. The large embedment, coupled with steel's capacity to dissipate energy when yielding, makes these piles suitable designs even against extremely large waves as they are likely to stay in place and reduce the tsunami's energy through yielding for overtopping, larger-than-designed-for waves.

Since the design of these seawall structures is mostly concerned with their capacity to withstand very powerful waves it can be considered a true Ultimate Limit State (ULS) design scenario. Currently evaluating the capacity of these seawalls employs design codes not specifically meant for this application.

By analysing the experimental data from a lateral loading test on a pile of the type used in the Kochi coast defences insight can be gained regarding how well the current design guides scale to large diameter stiff tubular structures.

2 CURRENT CODES OF PRACTICE

Modern design practice for predicting the lateral capacity of piles in sand is based on data from tests on flexible, 0:4m to 0:6m diameter piles published in the 1960's and 1970's in well known papers such as Broms (1964) and Reese et al. (1974).

Since soil displaces around a laterally loaded pile in a complex manner, lacking a known analytical expression, the general way to model soil-structure interaction has been to employ non-linear Winkler springs (Winkler 1867). These link the net soil pressure exerted on the pile at each depth $p(z)$ to the pile displacement $y(z)$ through a spring constant which varies with y, depth z, ground conditions and number of cycles. Knowing the $p-y$ relation is sufficient to derive the pile lateral response, including ultimate load and displacement.

An important requirement for the $p-y$ method is a good prediction of the ultimate soil pressure p_u. Most empirical p_u relations are of the form shown in eq.1.

DOI: 10.1201/9781003215226-18

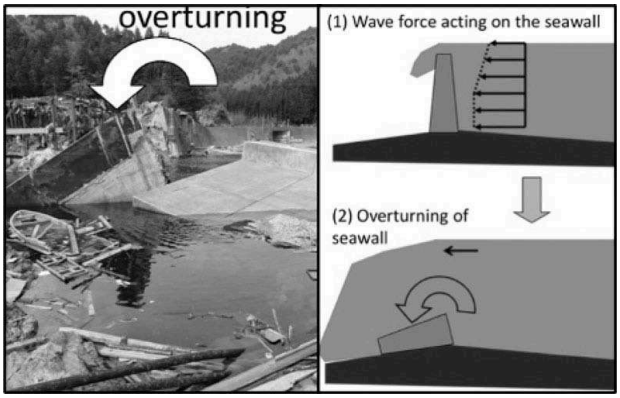

Figure 1. Seawall failure (Kato et al. 2012).

$$p_u = K_q \gamma' z D, \tag{1}$$

where K_q is an earth pressure coefficient depending on Φ (friction angle), γ' is the effective unit weight of soil and D is pile width or diameter. Broms (1964) proposed the following expression for K_q:

$$K_q = 3 \times K_p, \tag{2}$$

in which K_p is the passive earth pressure coefficient. Reese et al. (1974) advanced a different semi-empirical definition for K_q by assuming a wedge mechanism forming close to the ground surface and radial, 2D deformation dominating at significant depths:

$$K_q = K_p - K_a + \tfrac{z}{D}(K_p - K_0)\sqrt{K_p}\tan\alpha + \tfrac{z}{D}K_0\sqrt{K_p}\left(\tfrac{1}{\cos\alpha} + 1\right)\tan\Phi\sin\beta \tag{3}$$

near the surface and

$$K_q = K_p^3 + K_0 K_p^2 \tan\Phi - K_a \tag{4}$$

well below ground surface. K_a and K_0 are the active and in-situ earth pressure coefficients, $\beta = 45^\circ + \Phi/2$, α is wedge angle. The resulting K_q is then scaled by pure empirical parameters depending on z and D representing the deviation between eq.3-4 and the measured K_q in the tests conducted by Reese et al. (1974).

Two widely used design standards by Det Norske Veritas (DNV 1992) and the American Petroleum Institute(API 2000) feature a simplified version of Reese et al. (1974) based on a report by O'Neill and Murchinson (1983). The empirical factor A, defined by eq.5, is significantly simplified.

$$A = \left(3 - 0.8\frac{z}{D}\right)0.9 \tag{5}$$

Finally, the p – y relation as given in design codes (eq.(6)) is a hyperbolic function as opposed to the parabolic expression in Reese et al. (1974).

$$p = A p_u \tanh\left(\frac{kz}{A p_u} y\right) \tag{6}$$

k is the initial modulus of subgrade reaction and it is derived in DNV (1992) and API (2000) by identical methods based purely on Φ.

Hence by evaluating the in-situ conditions of our lateral loading test and knowing pile diameter, length and stiffness the predicted $p - y$ can be calculated from the above equations. These curves can be integrated to give predictions of pile deflection, bending moment and net soil pressure distribution which may be compared with experimental findings.

3 EXPERIMENTAL SETUP

The tests were carried out at Giken Ltd's Nidahama trial site in Kochi, Japan. Next to the Pacific, and within a mile from where the new piled seawalls were being actively deployed in Kochi, Nidahama provided ground conditions similar to the ones the production piles would be installed in. Sieve analysis was used to grade the Nidahama soil according to ASTM (2017). The result was a silty sand with 20% fines by mass bearing the SM designation. Table 1 summarises the ground properties at the test site, with further data from Nidahama found in Gillow et al. (2018).

Table 2 provides a summary of key pile properties as specified by the manufacturer.

Table 1. Derived soil properties at Nidahama site (Dobrisan et al. 2018).

Water table depth	γ_t	γ'	R_d	Φ_{crit}	Φ_{peak}
m	kN/m^3	kN/m^3	%	Deg	Deg
7.45	20	12.4	70	32	40

Table 2. Key data for the tested pile of type SKK490 (Dobrisan et al. 2018).

Diameter	Section Thickness	Pile Length	Embedment	Yield Stress	Tensile Stress
m	mm	m	m	MPa	MPa
1.0	22	15	10	315	490

A hydraulic jack was used to load the pile up to forces equal in magnitude to those a tsunami would apply on a seawall. A reaction system made up of four steel piles similar to the one being tested was used (Figure 2). The deflection of the reaction system was monitored during the test to ensure it was stiff enough not to affect the experiment.

A schematic of the experiment setup and of the instruments used is shown in Figure 3. The hydraulic jack position of 2.4m above the ground level was chosen to be similar to the point of application of the equivalent static wave force as dictated by Japanese codes (Okada et al. 2006).

The pile was instrumented with ten strain gauge pairs, each coupled with an inclinometer. These were placed at 1 intervals below ground. LVDTs and wire displacement sensors were used to infer pile movement at the ground level.

The pile was subjected to two load cycles, the maximum applied force being 1836, which coincided with the observed onset of yielding in the strain gauges.

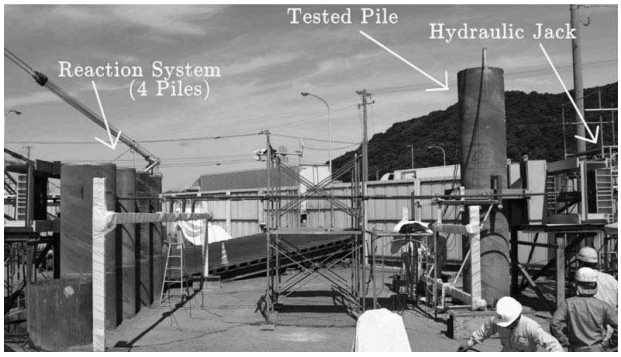

Figure 2. Lateral pile loading system (Dobrisan et al. 2018).

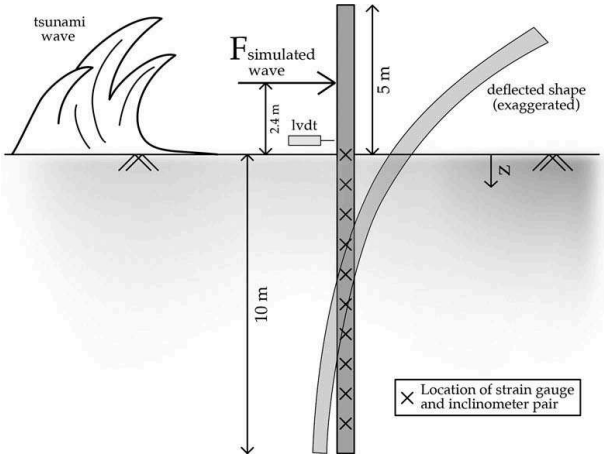

Figure 3. Schematic of pile loading and instrumentation. The pile head is free to move and rotate.

4 ANALYSIS METHOD

From the strain gauge measurements the moment profile along the depth at a given lateral load can be derived. The inclinometer data gives a measure of pile rotation. Since Euler-Bernoulli beam theory allows differentiating moment twice to get soil pressure p and integrating twice for pile displacement y, $p-y$ curves could be obtained from the strain gauge data alone. Similarly rotation data could be differentiated three times and integrated once to yield the same result. To differentiate and integrate the data fits need to be found connecting the discrete instrument measurements and giving continuous plots of M and θ (rotation) respectively. The errors in interpolating using standard techniques like polynomial or spline fitting compounded by measurement errors means obtaining $p-y$ results consistent between the strain gauge and inclinometer measurements could not be achieved. However, a different approach, named *multifit* (Dobrisan et al. 2020), enables obtaining reliable $p-y$ results from the noisy data set. In short, by specifying the errors for each instrument type, the method searches for the family of polynomial fits that satisfies all experimental measurements (strain gauges, inclinometers etc.) simultaneously within the given error bounds. Afterwards, the range of probable values for M, P, y etc. is taken as the interval between the 20th and 80th percentiles (Figure 4).

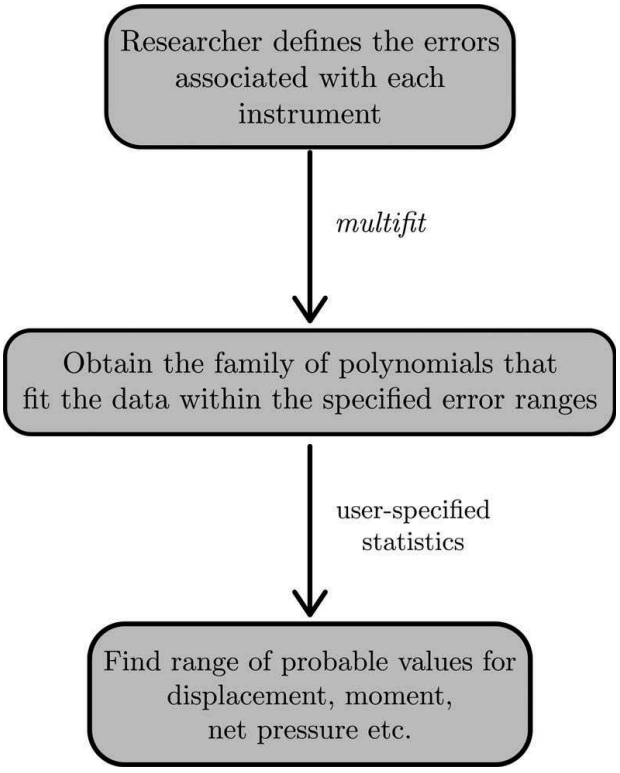

Figure 4. Diagram of *multifit* procedure (Dobrisan et al. 2020).

5 RESULTS. DISCUSSION

Figure 5 shows the measured load-displacement curve at the hydraulic jack location.

It can be seen that Reese et al. (1974) predicts the overall pile stiffnes to a high degree of accuracy with the API (2000) result predicting a somewhat stiffer response. Both numeric solution underpredict the ultimate load capacity of the pile by a considerable factor. To further compare the experimental results to the design code, *multifit* was used to derive the pile properties at each loading stage.

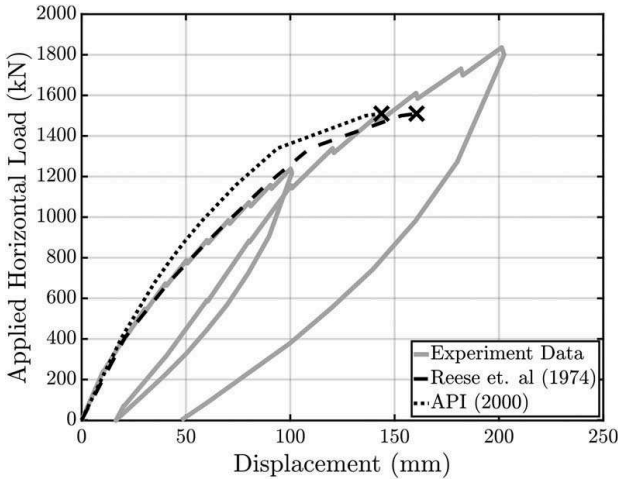

Figure 5. Load-displacement curve, experimental vs predicted.

A conservative overall relative error of 10% was considered for both strain gauges and inclinometers alike. The results are shown in Figure 6 for a representative hydraulic jack loading of 984kN, with the other loading stages generating comparable plots.

A first observation is that, even though the Reese et al. (1974) deflection curve is almost identical to the *multifit* result for the top 5m in Figure 6a, the predicted behaviour is very different to the *multifit* one at larger depths. Both the design codes and Reese analyses predict virtually no deflection at the base of the pile, whereas the fitted data suggests there is mobilisation at this level, with a rotation point present in the pile just above 6m depth. Due to the high confining stress around the base of the pile this toe movement generates significant soil pressure as shown in Figure 6e. The numeric predictions show negligible p at the pile base ($z = 10$) consistent with the prediction of zero deflection at this point. However, the significant soil pressure at depth predicted by multifit aligns well with the measured moment data as the increased base resistance brings down the peak bending

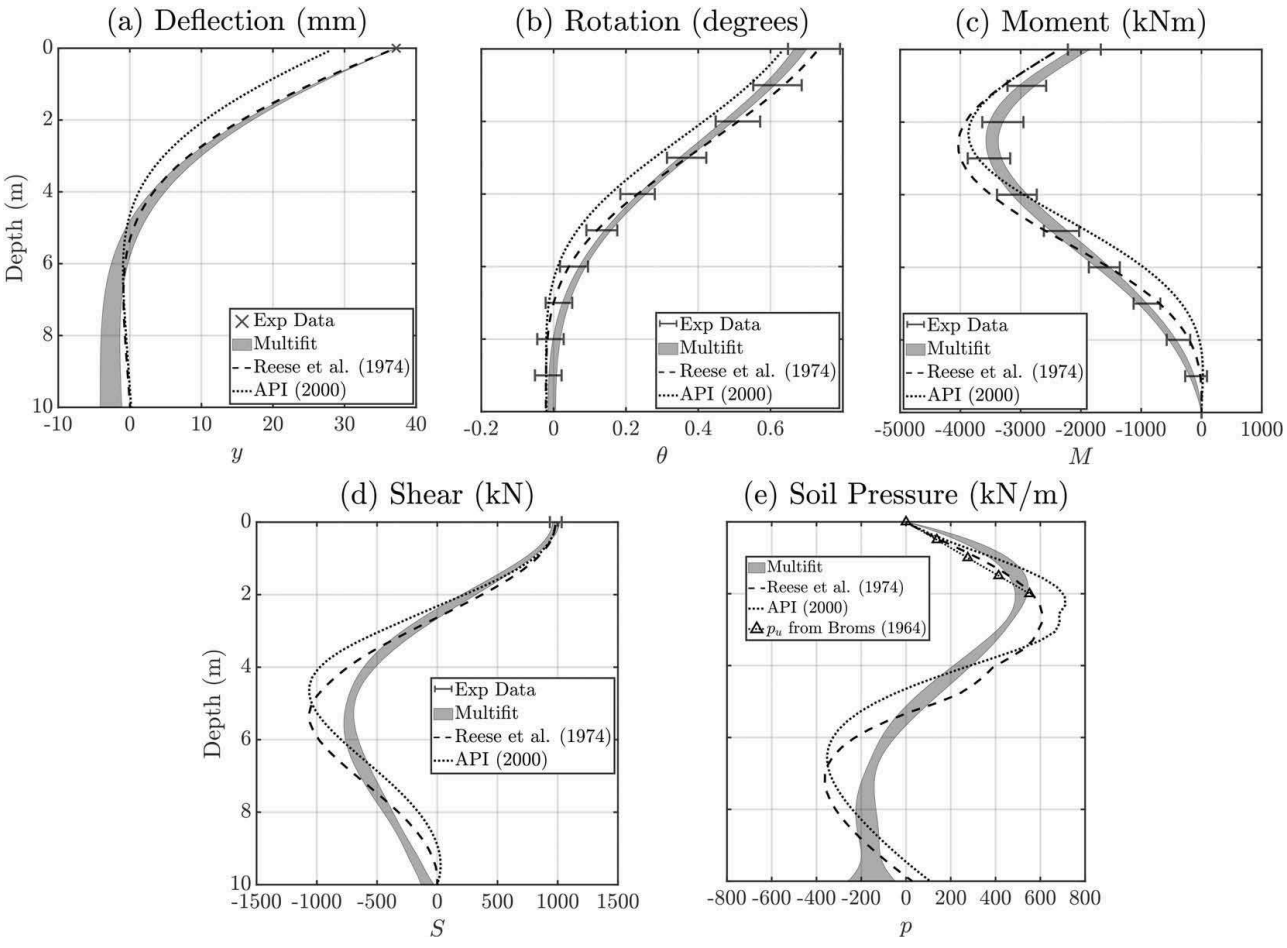

Figure 6. Comparison between multifit results and current codes at 984kN loading.

moment compared to the numeric results, with both overshooting the measured value. The shear plot in Figure 6d consolidates the observation that mobilising the deeper soil strata leads to a reduction of the bending stress on the pile, which may potentially explain the larger than predicted ultimate load measured. This mobilisation of deeper layers does not seem to be captured by current codes, potentially due to the fact that the flexible piles on which they were based lacked sufficient rigidity to move the toe of the pile.

Since most of the soil was not mobilised enough to reach p_u, comparing the K_q predictions is restricted to the very shallow top 1.5m of soil where failure occurred. It can be seen that both Broms (1964) and Reese et al. (1974) underpredict the ultimate capacity of the soil. However, the correction codes like DNV (1992) and API (2000) make on K_q through factor A (eq.5) seems to move the prediction significantly closer to the experimentally deduced gradient at shallow depths.

By using the p and y data from *multifit* across each loading stage, the experimental $p-y$ curves can be predicted. Figure 7 plots $p-y$ at 2m depth. p_u is not reached at this location and the experimental results show a slightly less stiff response than Reese et al. (1974) predicts. Even though both numeric results have the same initial stiffness and similar p_u the fact that API (2000) replaces the parabola in Reese et al. (1974) with a hyperbolic (eq. 6) seems to have detrimentally affected the stiffness estimate. A significantly larger error with respect to the experimental data is seen in the API (2000) prediction than in the Reese et al. (1974) one.

With increasing depth (Figures 8 and 9) it can be seen that the numerical results start to significantly overpredict the stiffness of the soil response. At all measured depths past 3 the same behaviour of

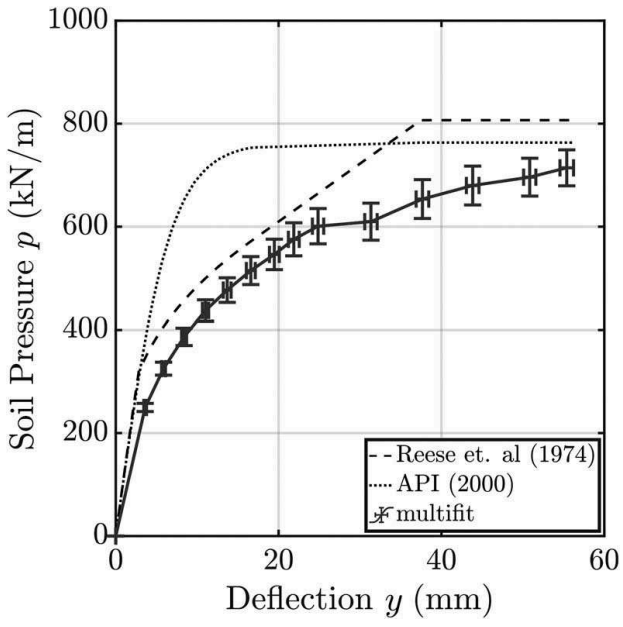

Figure 7. $p-y$ result at 2m depth.

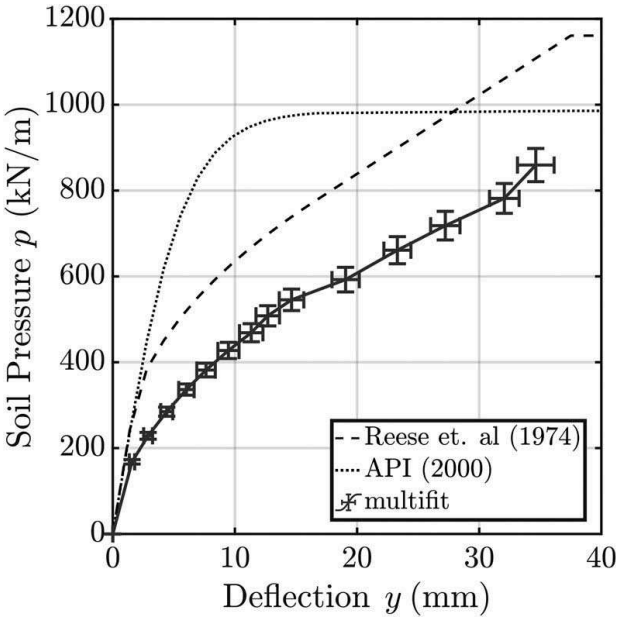

Figure 8. $p-y$ result at 3m depth.

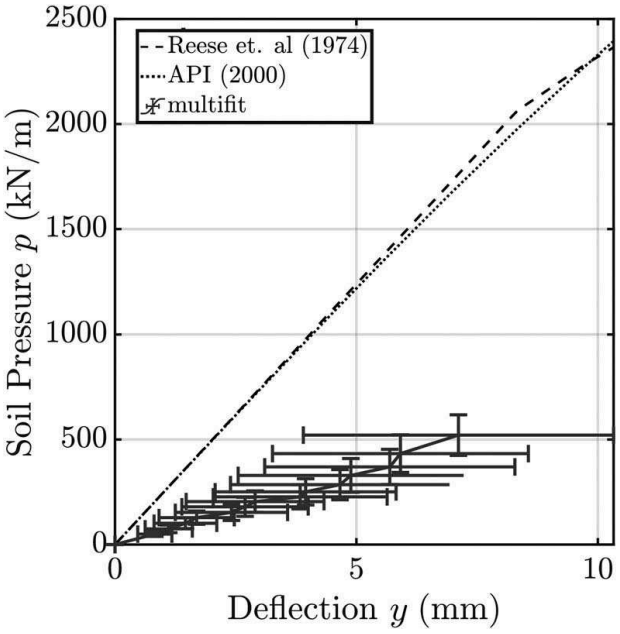

Figure 9. $p-y$ result at 8m depth.

numerical overprediction was found. Conceptually this correlates well with earlier remarks: a stiffer soil has less compliance and thus more of the lateral load has to be carried by the pile which leads to the design codes underpredicting the load carrying capacity of the pile-soil system.

These experimental observations suggest there are significant positive aspects to the highly embedded, tubular pile seawall design. It was shown that by mobilising the soil at depth these structures can carry more load than design calculations suggest. The mechanism of spreading the load out to the deep soil strata is especially encouraging since the

incoming wave might erode some of the top soil layers and significantly decrease the load carrying capacity of the shallower layers.

6 CONCLUSIONS

The usual engineering practice of designing a structure for a given return period of a natural hazard might have to be rethought considering the extremely large, unpredictable hazards in recent memory such as the Tōhoku earthquake and tsunami. Further global climate change might make these super-events even more likely and a new mindset is required to prevent tragic losses. Engineering structures ought to behave well not only for designed scenarios, but should have a beneficial role even for loads much larger than those that could be reasonably expected.

A seawall design of stiff, large diameter, adjoined steel tubular piles was discussed as a possible replacement for traditional concrete caisson structures. Benefits include a higher embedment, piles being unlikely to be 'washed-off' by the wave, and capacity to dissipate wave energy through yielding.

Designing such a pile wall requires knowledge of the soil-structure interaction and design codes are shown to include empirical relations based on experiments on smaller and more flexible piles. A lateral loading test was discussed and the experimental results were compared with numerical predictions using design code equations. A novel fitting method, *multifit*, was used to get improved insight from the recorded data and allow for measurement errors.

It was found that design codes tend to predict large soil stiffness increase with depth and thus imply very little pile toe movement during deformation. This means the bulk of the load has to be carried in the shallower depths which translates to decreased load carrying capacity and potential issues during a tsunami event, as the wave may erode the top soil and weaken the shallow layers. However, the data analysis shows the soil stiffness is significantly less than the code predictions. This implies the deeper soil layers are mobilised and the pile toe can move. The result is significantly less loading on the pile and a higher measured ultimate capacity than prediction. The fact that the deeper soil is mobilised is encouraging since these layers are less likely to significantly weaken during a wave collision.

Overall it was found that the pile wall design has improved geotechnical properties for withstanding wave loading when compared to concrete caissons and that design codes might have to be adjusted to account for the larger diameter piles being used presently in seawalls, wind turbines etc.

7 MULTIFIT ROUTINE

The *multifit* procedure of analysing experimental data from retaining wall and lateral pile tests has been implemented in MATLAB and is freely accessible at gitlab.developers.cam.ac.uk/ad622/multifit. Documentation and worked examples are made available at the link above to facilitate the use of *multifit* in geotechnical research.

ACKNOWLEDGEMENTS

The authors are grateful to EPSRC for support in the form of a Doctoral Training Award to A.D, grant number EP/M508007/1. The support of Giken Ltd. in providing the data from the pile lateral loading experiment is gratefully acknowledged.

REFERENCES

API (2000). Recommended Practice for Planning, Designing and Constructing Fixed Offshore Platforms-Working Stress Design. Technical Report 2A-WSD.

ASTM (2017). Standard Practice for Classification of Soils for Engineering Purposes (Unified Soil Classification System). Technical Report D2487, ASTM International.

Broms, B. B. (1964). Lateral Resistance of Piles in Cohesionless Soils. *Journal of the Soil Mechanics and Foundations Division 90*(3), 123–158.

DNV (1992). Foundations. Technical Report 30.4, Det Norske Veritas.

Dobrisan, A., S. K. Haigh, C. Deng, & Y. Ishihara (2020). Analysis of the behaviour of retaining structures through a novel data interpretation approach. *Unpublished*.

Dobrisan, A., S. K. Haigh, & Y. Ishihara (2018). Evaluating the Efficiency of Jacked-in Piles as Tsunami Defences. In *The First International Conference on Press-in Engineering*, Volume 1, Kochi, Japan, pp. 289–296. International Press-In Association.

Gillow, M., S. K. Haigh, & Y. Ishihara (2018). Water Jetting for Sheet Piling. In *The First International Conference on Press-in Engineering*, Volume 1, Kochi, Japan, pp. 335–342. International Press-In Association.

Kato, F., Y. Suwa, K. Watanabe, & S. Hatogai (2012). Mechanisms of coastal dike failure induced by the Great East Japan Earthquake Tsunami. *Coastal Engineering Proceedings 1*(33).

Okada, T., T. Sugano, T. Ishikawa, S. Takai, & T. Tateno (2006). Tsunami loads and structural design of tsunami refuge buildings. *The Building Centre of Japan*.

O'Neill, M. & J. Murchinson (1983). Fan evaluation of p-y relationships in sands. Technical report, American Petroleum Institute.

Reese, L. C., W. R. Cox, & F. D. Koop (1974). Analysis of laterally loaded piles in sand. In *Sixth Annual Offshore Technological Conference*, Houston, Texas, pp. 473–483.

Winkler, E. (1867). *Theory of elasticity and strength*. Prague: Dominicus.